Adhikari et al., http://www.jcb.org/cgi/content/full/jcb.201406033/DC1

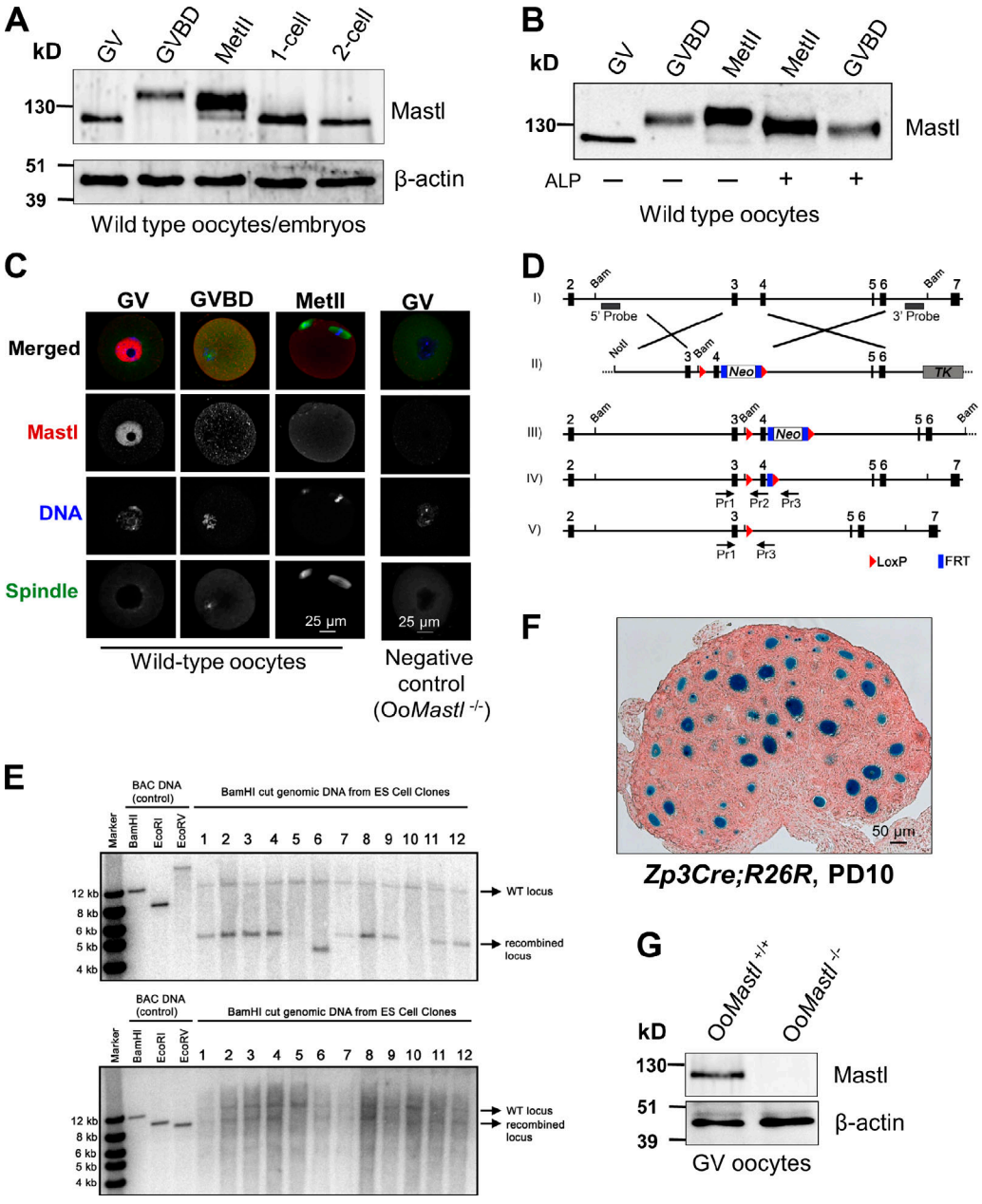

Figure S1. **Phosphorylation and localization of Mastl in mouse oocytes and generation of *Mastl* conditional knockout mice.** (A) Immunoblotting for Mastl during oocyte maturation and in early embryos. (B) Mobility shift of Mastl after the treatment of wild-type oocyte lysates with alkaline phosphatase (ALP). (C) Mastl was localized in the GV before meiotic resumption but was found throughout the ooplasm of the oocytes at the GVBD and MetII stages. Oo*Mastl*$^{-/-}$ oocytes were used as negative controls. 30 oocytes per group were analyzed, and representative images are shown. (D) The murine *Mastl* genomic locus (I) was modified in ES cells with the targeting vector (II). An FRT-flanked (blue rectangles) neomycin-selection cassette was introduced along with two *LoxP* recombination sites (red triangles) on both sides of exon 4, and this generated a mutant *Mastl* locus (III). For Southern blot analysis, 5′ and 3′ probes located outside of the targeting vector were used as above. BamHI digestion yields a 12.5-kb fragment in the wild-type locus and a 5.1-kb (detectable by the 5′ probe) and 9.1-kb (detectable by the 3′ probe) fragment in the homologous recombined locus. Upon expression of FLP recombinase, the neomycin cassette is removed and only the *LoxP* sites flanking exon 4 remain in the locus (IV, *Mastl*^{FLOX}). Cre recombinase expression leads to excision of exon 4 (V), and this results in total deletion of the *Mastl* gene product caused by a frame shift. PCR genotyping primers are indicated (Pr1, Pr2, and Pr3), and the sequences can be found in Table S1. (E) Genomic DNA isolated from double-selected ES cell colonies was digested with BamHI and analyzed by Southern hybridization using a 5′ probe (PKO721/PKO722, 500 bp). Homologous recombination at the 5′ site yields a 5.1-kb fragment (top). Genomic DNA was analyzed as above using a 3′ probe (PKO756/757, 600 bp). Homologous recombination at the 3′ site yields a 9.1-kb fragment. One of the ES cell clones (clone 3) that had undergone homologous recombination at both the 5′ and 3′ sites of exon 4 was selected for generation of the chimera (bottom). (F) β-Galactosidase staining (blue) in oocytes showing the high efficiency and specificity of the *Zp3-Cre* mouse line. (G) Oocyte-specific deletion of Mastl. For A, B, and G, lysate from 100 oocytes or embryos was loaded in each lane. The levels of β-actin were used as the control.

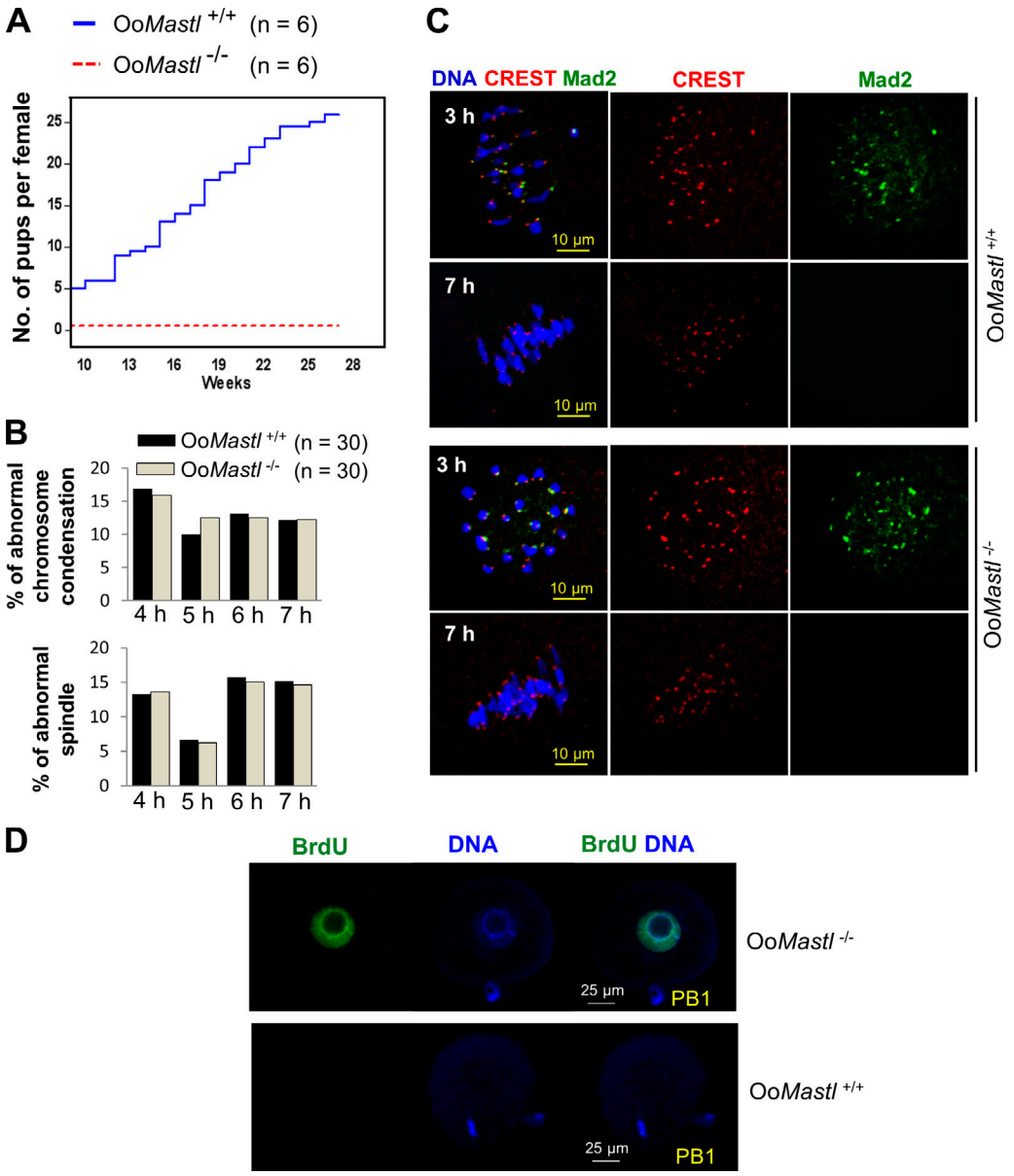

Figure S2. **Infertility of *Mastl* conditional knockout females, normal spindle and chromosome condensation, Mad2 dissociation from kinetochores, and BrdU incorporation in oocytes.** (A) Comparison of the cumulative number of pups per Oo*Mastl*$^{-/-}$ female (red dotted line) and per Oo*Mastl*$^{+/+}$ female (blue line). All Oo*Mastl*$^{-/-}$ females were infertile. Number of females monitored (n) is shown. (B) Comparison of the percentages of oocytes with abnormal spindle formation and abnormal chromosome condensation. Oocytes were cultured in vitro for the indicated periods after GVBD before staining for chromosomes, spindles, and kinetochores. (C) Representative images of immunostaining for DNA, CREST, and Mad2. Oocytes were fixed for immunostaining at either 3 or 7 h after GVBD. 30 oocytes were analyzed for each time point. (D) BrdU incorporation into decondensed chromatin of Oo*Mastl*$^{-/-}$ oocytes after PBE. The experiment was conducted three times using at least 10 oocytes per group, and representative images are shown.

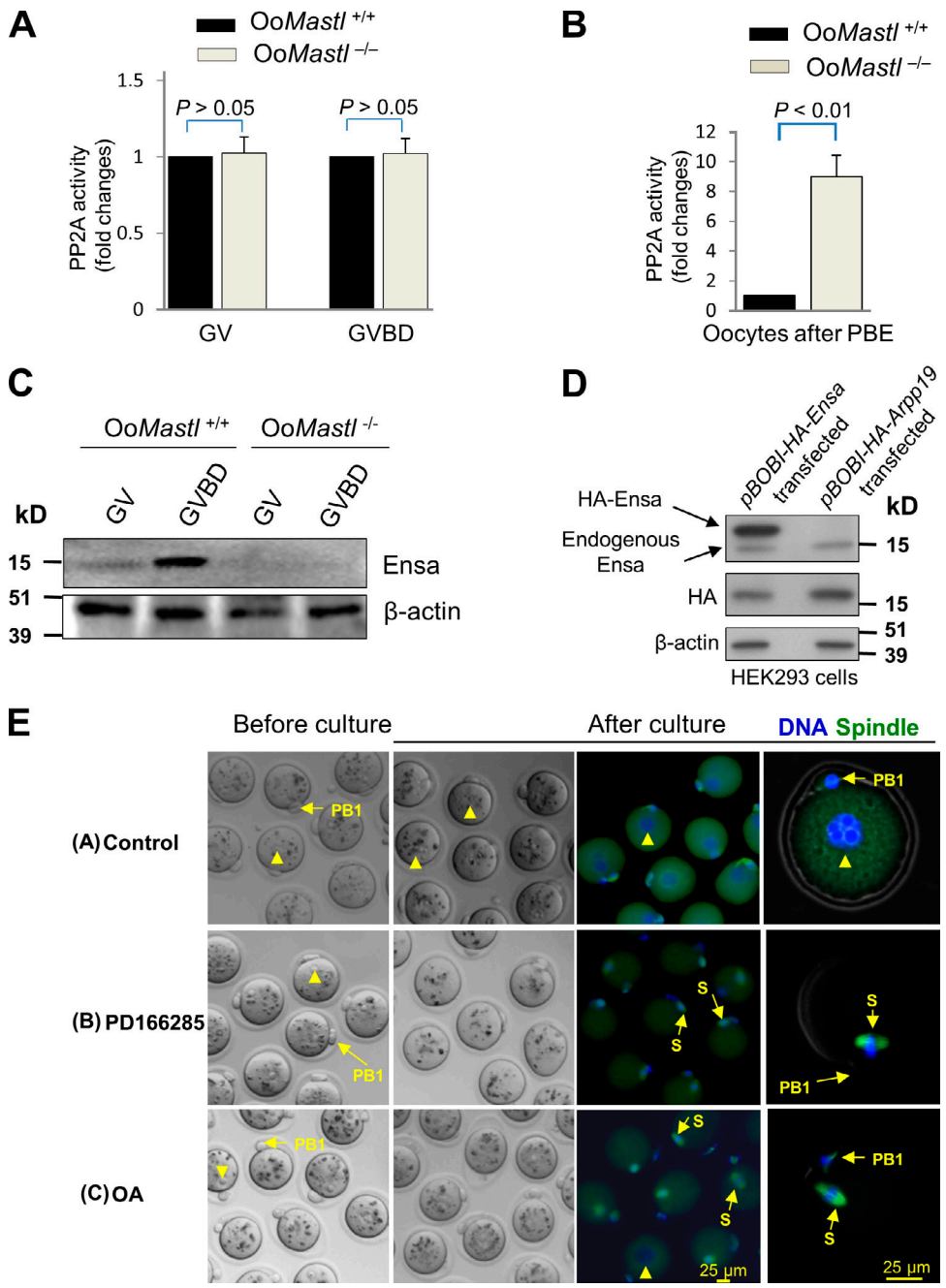

Figure S3. **PP2A activities and Ensa protein levels during oocyte maturation.** (A) Comparable PP2A activities in meiosis I in Oo*Mastl*$^{-/-}$ and Oo*Mastl*$^{+/+}$ oocytes. (B) Significantly elevated PP2A activity in Oo*Mastl*$^{-/-}$ oocytes after PBE ($P < 0.01$). For A and B, lysate from 400 oocytes was used for each time point, and error bars represent SD. The PP2A activity in the Oo*Mastl*$^{+/+}$ oocytes was set as 1.0, and fold changes in Oo*Mastl*$^{-/-}$ oocytes are shown. All experiments were repeated at least three times. The activity of PP2A immunoprecipitated by anti-PP2A antibody (specific to the catalytic subunit of PP2A) was related to the amount of inorganic phosphate released by dephosphorylating the phosphopeptide K-R-pT-I-R-R. (C) Expression of Ensa in GV and GVBD oocytes. (D) Validation of the specificity of the Ensa antibody (#8770; Cell Signaling Technology). The antibody specifically detects overexpressed HA-Ensa protein but does not cross-react with the HA-Arpp19 protein. As a control, anti-HA antibodies detect both the HA-Ensa and HA-Arpp19 proteins in the transfected HEK293 cells. The levels of β-actin were used as a loading control. In each lane, 10 μg cell lysate was loaded, and representative results of three repeated experiments are shown. (E) A representative experiment for obtaining data for Fig. 4. Before treatment with inhibitors, all of the oocytes contained a nucleus (arrowheads) and a PB1. Immunofluorescence of Oo*Mastl*$^{-/-}$ oocytes treated with inhibitors indicating formation of spindles (S) and chromosome condensation. All experiments were repeated at least three times, and representative results are shown.

Table S1. **PCR genotyping primers**

Primer name	Primer sequence
5′ Probe Forward, PKO721	5′-TTGGTGATTATATTGTTAATGAAACTG-3′
5′ Probe Reverse, PKO722	5′-AAAAAAGGATTACGGATTACAAAGCTTC-3′
3′ Probe Forward, PKO756	5′-CCTAGTTGTAAAACGTAATGCTTA-3′
3′ Probe Reverse, PKO757	5′-AGGGATCCCTGTCCCTATCTTTA-3′
Genotyping Pr1, PKO860	5′-CATGCCTTCCTTGAAAGAGGTGGAC-3′
Genotyping Pr2, PKO862	5′-GTGGGAGGAATTACAAGAGACAAC-3′
Genotyping Pr3, PKO863	5′-GGCAGGTGGAGGCAAGAGCTCACAGA-3′

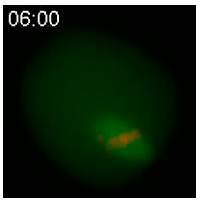

Video 1. **Live imaging showing the normal MII entry in Oo*Mastl*$^{+/+}$ oocytes.** Oo*Mastl*$^{+/+}$ oocytes at the GV stage were microinjected with mRNAs to allow the expression of H2B-mCherry (red fluorescence for labeling DNA) and Map7-EGFP (green fluorescence for labeling spindle microtubules). The oocytes were cultured for 6 h after GVBD when the oocytes reached the metaphase I stage. Images were analyzed by epifluorescence live cell time-lapse microscopy using a DMI6000 B microscope equipped with an HCX PL FLUOTAR 20×/0.40 CORR objective, dichroic filters L5 and TX2, a heating stage at 37°C, and a stage cover maintaining 5% CO_2. Images were taken every 15 min for 16 h with an ORCA-ER charge-coupled device camera operated by MetaMorph software. In seven independent experiments, a total of 30 Oo*Mastl*$^{+/+}$ oocytes were analyzed. In this particular experiment, Oo*Mastl*$^{+/+}$ oocytes established metaphase I (07:15), extruded the PB1 (anaphase I), subsequently reformed bipolar spindles (prometaphase II), and aligned chromosomes again (MetII).

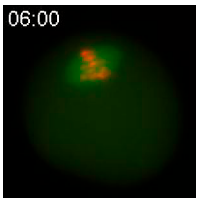

Video 2. **Live imaging showing the failure of MII entry in Oo*Mastl*$^{-/-}$ oocytes.** Oo*Mastl*$^{-/-}$ oocytes at the GV stage were microinjected with mRNAs to allow the expression of H2B-mCherry (red fluorescence for labeling DNA) and Map7-EGFP (green fluorescence for labeling spindle microtubules). The oocytes were cultured for 6 h after GVBD when the oocytes reached the metaphase I stage. Images were analyzed by epifluorescence live cell time-lapse microscopy using a DMI6000 B microscope equipped with an HCX PL FLUOTAR 20×/0.40 CORR objective, dichroic filters L5 and TX2, a heating stage at 37°C, and a stage cover maintaining 5% CO_2. Images were taken every 15 min for 16 h with an ORCA-ER charge-coupled device camera operated by MetaMorph software. In seven independent experiments, a total of 14 Oo*Mastl*$^{-/-}$ oocytes were analyzed. The Oo*Mastl*$^{-/-}$ oocytes also established metaphase I (07:15), but upon completion of chromosome segregation, the chromosomes were decondensed, leading to nucleus reformation. Chromosomes were not recondensed and microtubules did not reform bipolar spindles during the observation period, suggesting that completion of meiosis I was followed by an interphase without any observable indication of MII in Oo*Mastl*$^{-/-}$ oocytes.